Progress In Electromagnetics Research, Vol. 154, 181–193, 2015

Review of Black Hole Realization in Laboratory Based on Transformation Optics

Shahram Dehdashti[1], Huaping Wang[2], Yuyu Jiang[1], Zhiwei Xu[2], and Hongsheng Chen[1, *]

(*Invited Paper*)

Abstract—Realizations of celestial objects in the laboratory have been a tantalizing subject for human beings over centuries. In this paper, we review some of the interesting cases of realizations of black holes in the laboratory. We first review the recent progress in observed black holes realized through the isotropic coordinate transformation method, then discuss the realization of optical attractors. Finally, the Rindler space-time, as a one-dimensional black hole, by using the hyperbolic metamaterials, is discussed.

1. INTRODUCTION

Undoubtedly, general relativity has been an interesting field of science. Indeed, general relativity has changed the human view of the world as well as advanced geometrical methods in theoretical physics. Moreover, increased understanding of curved space-time has been additional motivation for the investigation of objects such as black holes, worm holes, FRW universe, etc. [1]. In these investigations, the existence of singularity, event horizon, thermodynamic properties and absorption of everything have defined black holes in particular as an interesting subject. Ability to generate black holes in the laboratory has technical application in solar energy harvesting photovoltaic systems, thermal light emitting sources, optoelectronic devices, etc. [2–4].

Realization of black holes is possible from two perspectives. On the one hand, it is theoretically related to transformation optics, based on the equivalent of curved space-time and material, which leads to control and engineering of electromagnetic waves [5–9]. On the other hand, realization is experimentally related to metamaterial science as is a result of progresses in the engineering of material properties which have led to the study and creation of general relativitys objects. With these two perspectives as points of venture, the collected studies first incorporate different theoretical methods and fields of study in physics, including general relativity, condensed matter, optics, etc. [10–16]; second, discuss the aforementioned experimental progresses to demonstrate the celestial objects such as black holes, worm holes, FRW universe and Gödel universe, etc. in the laboratory [16–37]; and third, illustrate the curved space-time and two-time physics realizations in hyperbolic metamaterials to invite discussion for the advancement of theoretical physics [38–45]. Two challenging opportunities for continued research in this field of study present themselves: first, deeper theoretical understanding of curved space-time transformation optics as well as realization in hyperbolic metamaterials, which would improve upon current understanding of curved space transformation optics [46–49]; second, progress in the engineering

Received 25 November 2015, Accepted 22 December 2015, Scheduled 31 December 2015
Invited paper for the Commemorative Collection on the 150-Year Anniversary of Maxwell's Equations.
* Corresponding author: Hongsheng Chen (hansomchen@zju.edu.cn).
[1] The Electromagnetics Academy at Zhejiang University, Zhejiang University, Hangzhou 310027, China. [2] Ocean College, Zhejiang University, Hangzhou 310058, China.

of metamaterial refractive indexes which would support future realization of celestial objects in the laboratory with properties as close to the original objects as possible [46].

As is mentioned, the black hole is one of the interesting subjects in the physics due to the existence of singularity, event horizon and thermodynamic properties as well as its relation to quantum information, quantum gravity and string theory [50]. Indeed, realization of a black hole in the laboratory has be suggested for at least two reasons: first, extension and verification of theoretical studies of black hole properties such as Hawking radiation in the event horizon [11, 51, 52]; second, generation of optical black hole, or attractor, for use in control of electromagnetic waves in technological applications; the subject which is reviewed in this paper.

In this review, we start with the Maxwell equations in curved space-time, which when applied to the isotropic metric of the Schwarzschild black hole, gives the refractive index of equivalent medium. This structure is too complicated to realize, therefore a cylindrical Schwarzschild black hole is considered, which despite the fact that it is easier to realize in comparison to the former, it has two main challenges: first, it is infinitely large; second, anisotropic materials are needed for its realization. In the following, we study the suggested manners to solve these challenges. Then, we review the optical black hole, attractor, in detail, based on the papers that have been published so far. Also, we mention the experimental work that has been done in studies of the optical attractor. Finally, we consider Rindler space-time, as a one dimensional black hole, as realized through hyperbolic metamaterials.

2. ELECTROMAGNETIC WAVES IN SCHWARZSCHILD BLACK HOLE

The source-free Maxwell equations, in the covariant formalism, are written by [53]

$$\begin{aligned} d\mathbf{F} &= 0, \\ d \star \mathbf{F} &= 0, \end{aligned} \tag{1}$$

where the Hodge star operator $\star$, by using the antisymmetric Levi-Civita symbol $\epsilon_{\alpha\beta\sigma\rho}$, is defined by [53]

$$\star_{\alpha\beta}{}^{\mu\nu} = \frac{1}{2}\sqrt{|g|}\epsilon_{\alpha\beta\sigma\rho}g^{\sigma\mu}g^{\rho\nu}, \tag{2}$$

and

$$\mathbf{F} = \begin{pmatrix} 0 & -E_x & -E_y & -E_z \\ E_x & 0 & B_z & -B_y \\ E_y & -B_z & 0 & B_x \\ E_z & B_y & -B_x & 0 \end{pmatrix}. \tag{3}$$

Now, by using $H^{\mu\nu} = \sqrt{|g|}F^{\mu\nu}$, the Maxwell equations can be written as [54],

$$\begin{aligned} H^{\mu\nu}{}_{,\nu} &= 0, \\ \star\, H^{\mu\nu}{}_{,\nu} &= 0, \end{aligned} \tag{4}$$

In this case, component of $H^{\mu\nu}$ is defined by following relations [54]:

$$\mathbf{H} = \begin{pmatrix} 0 & -D_x & -D_y & -D_z \\ D_x & 0 & H_z & -H_y \\ D_y & -H_z & 0 & H_x \\ D_z & H_y & -H_x & 0 \end{pmatrix}. \tag{5}$$

It is evident that relations (4) are similar to the Maxwell equations in the flat space, on the following constitutive condition [54],

$$\begin{aligned} D_i &= \varepsilon_{ik}E_k - (\mathbf{G}\times\mathbf{H})_i, \\ B_i &= \mu_{ik}H_k - (\mathbf{G}\times\mathbf{E})_i \end{aligned} \tag{6}$$

where

$$\begin{aligned} \varepsilon_{ik} &= \mu_{ik} = -\sqrt{|g|}\frac{g^{ik}}{g_{00}} \\ G_i &= \frac{g_{i0}}{g_{00}}. \end{aligned} \tag{7}$$

Therefore, the Maxwell equations in the flat space that is filled with media are similar to the Maxwell equations in the curved space-time, i.e., geometries appear as dielectric media [54].

Now, let us start with the Schwarzschild black hole metric, defined as follows:

$$ds^2 = -\left(1-\frac{r_s}{r}\right)dt^2 + \left(1-\frac{r_s}{r}\right)^{-1}dr^2 + r^2 d\theta^2 + r^2\sin^2\theta d\phi^2, \tag{8}$$

in which Schwarzschild radius $r = r_s$ has the well-behaved and finite curvature tensors, but the space-time has a horizon in these coordinates [53]. As mentioned, we have to write the Maxwell equations in the Cartesian coordinates. For this purpose, we introduce the isotropic metric form:

$$ds^2 = -\left(1-\frac{r_s}{f(\rho)}\right)dt^2 + \left[\frac{f(\rho)}{\rho}\right]^2\left(d\rho^2+\rho^2 d\theta^2+\rho^2\sin^2\theta d\phi^2\right) = -\left(1-\frac{r_s}{f(\rho)}\right)dt^2 + \left[\frac{f(\rho)}{\rho}\right]^2\left(\delta_{ij}dx^i dx^j\right), \tag{9}$$

which

$$x = \rho\cos\phi\sin\theta, \quad y = \rho\sin\phi\sin\theta, \quad z = \rho\cos\theta, \tag{10}$$

and ρ is the isotropic radial coordinate. Now, we impose the condition $r = f(\rho)$ so that the metric (8) is turned into metric (9). This relation imposes the following relation:

$$\rho\frac{df}{d\rho} = \sqrt{f^2 - fr_s}. \tag{11}$$

Therefore, by using (7), we can obtain:

$$n = \varepsilon^{ij} = \mu^{ij} = \frac{f(\rho)}{\rho}\frac{1}{\sqrt{1-\frac{r_s}{f(\rho)}}} = \frac{1}{2}\frac{\left(1+\frac{r_s}{2\rho}\right)^3}{\left(1-\frac{r_s}{2\rho}\right)}\delta_{ij}. \tag{12}$$

In the approximation of geometrical optics, i.e., the dielectric permittivities do not vary significantly over the local wavelength, the effective Hamiltonian, which describes the trace of light ray, is given by [23],

$$\mathcal{H}_{eff} = \frac{p_\rho^2}{2\varepsilon(\rho)} + \frac{m^2}{2\rho^2\varepsilon(\rho)}, \tag{13}$$

where p_ρ is the radial momentum and m the total angular momentum. A straightforward solution of the Hamiltonian equations for Equation (13) yields the ray trajectories in the polar coordinates

$$\phi(\rho) = \phi_0 + \int_{m/\rho_0}^{m/r}\frac{d\xi}{\sqrt{C_0\varepsilon\left(\frac{m}{\xi}\right)-\xi^2}} \tag{14}$$

where the constants ρ_0, ϕ and C_0 are set by the initial conditions. Fig. 1(a) indicates the density plot of the refractive index (12) and ray path of light. Note that the isotropic radial coordinate ρ has no direct physical meaning.

The linearized Schwarzschild black hole is the another case which is described in this case [31]. Indeed, the linearized Schwarzschild black hole is an approximate solution of Einstein field equation and correspondence to the star's metric [55]:

$$ds^2 = -c^2\left(1-\frac{r_s}{r}\right)dt^2 + \left(1+\frac{r_s}{r}\right)\left(dx^2+dy^2+dz^2\right). \tag{15}$$

Moreover, another type of the linearized Schwarzschild black hole can be written as [56, 57],

$$ds^2 = -c^2\left(1-2\frac{r_s}{r}\right)dt^2 + dx^2 + dy^2 + dz^2. \tag{16}$$

The refractive indexes of both metrics, i.e., relations (15) and (16), by using relation (7), are respectively given by

$$\begin{aligned} n &= \sqrt{\frac{r+r_s}{r-r_s}}, \\ n &= \sqrt{\frac{r}{r-2r_s}} \end{aligned} \tag{17}$$

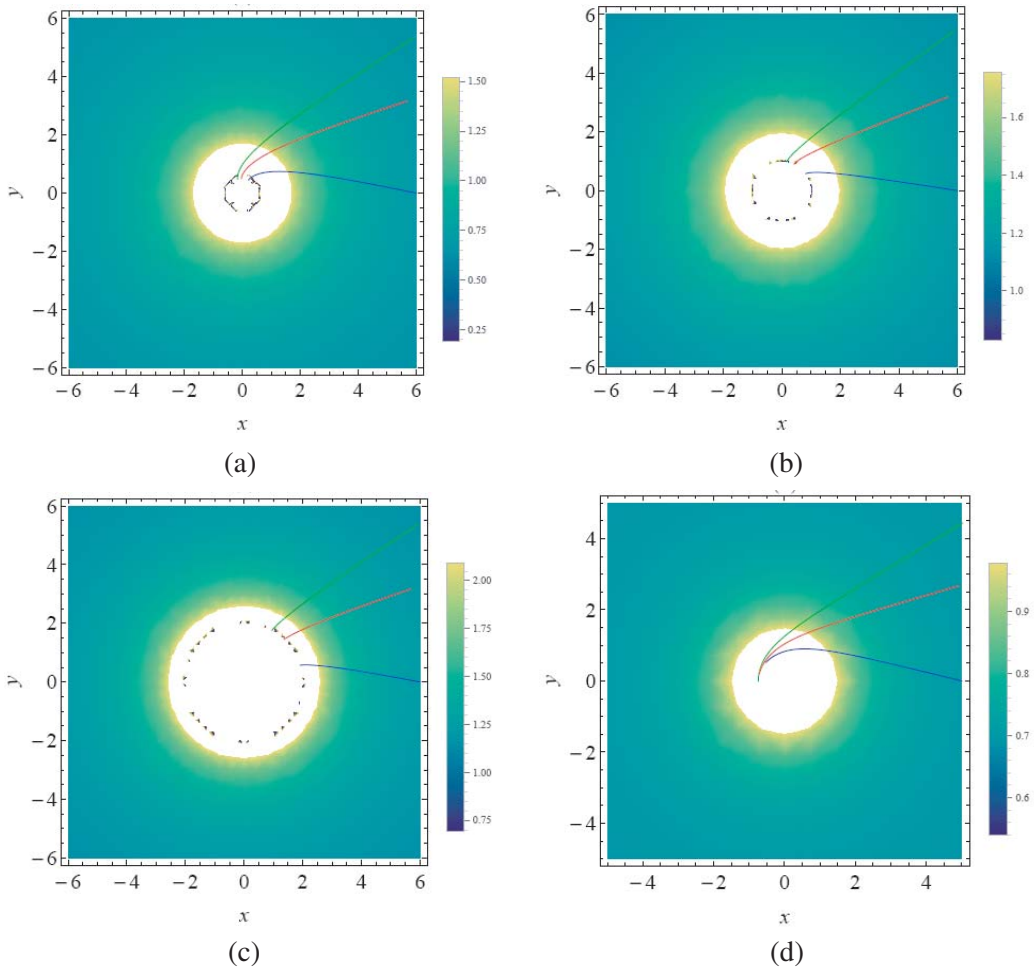

Figure 1. Density plots of refractive index of analogue medium of Schwarzschild black hole (12) and linearized Schwarzschild black holes (17), and (30) as well as propagation dynamics of light rays in plot (a), (b), (c) and (d), respectively.

which are respectively plotted in Figs. 1(b) and (c). Also, some paths of propagation light are plotted in these plots. It is obvious that refractive indexes in all cases diverge as the radial coordinate approaches the event horizon r_s and $2r_s$, in relations (12) and (17).

Also, by rewriting the Schwarzschild black hole in Cartesian coordinates [34],

$$g = \begin{pmatrix} -\left(1-\frac{r_s}{r}\right) & 0 & 0 & 0 \\ 0 & 1+\frac{r_s}{r-r_s}\frac{x^2}{r^2} & \frac{r_s}{r-r_s}\frac{xy}{r^2} & \frac{r_s}{r-r_s}\frac{xz}{r^2} \\ 0 & \frac{r_s}{r-r_s}\frac{xy}{r^2} & 1+\frac{r_s}{r-r_s}\frac{y^2}{r^2} & \frac{r_s}{r-r_s}\frac{yz}{r^2} \\ 0 & \frac{r_s}{r-r_s}\frac{xz}{r^2} & \frac{r_s}{r-r_s}\frac{yz}{r^2} & 1+\frac{r_s}{r-r_s}\frac{z^2}{r^2} \end{pmatrix}. \tag{18}$$

By using $\mathrm{M}^T g \mathrm{M}$, in which the orthogonal matrix M transfers the Cartesian coordinates to the spherical ones and is introduced by

$$\mathrm{M} = \begin{pmatrix} 1 & 0 & 0 & 0 \\ 0 & -\frac{x}{r} & \frac{z}{\sqrt{x^2+z^2}} & \frac{xy}{r\sqrt{x^2+z^2}} \\ 0 & -\frac{y}{r} & 0 & -\frac{\sqrt{x^2+z^2}}{r} \\ 0 & -\frac{z}{r} & \frac{-x}{\sqrt{x^2+z^2}} & \frac{yz}{r\sqrt{x^2+z^2}} \end{pmatrix}, \tag{19}$$

the diagonal transformation of the Schwarzschild black hole, in the spherical coordinates, is given as:

$$[g_{\alpha\beta}] = \text{diag}\left(-\left(1-\frac{r_s}{r}\right), \left(1-\frac{r_s}{r}\right)^{-1}, 1, 1\right). \tag{20}$$

Therefore, the tensor of permittivity, in the spherical coordinates, is given by

$$\varepsilon^{ij} = \text{diag}\left(1, \left(1-\frac{r_s}{r}\right)^{-1}, \left(1-\frac{r_s}{r}\right)^{-1}\right), \tag{21}$$

which describes an uni-axial dielectric-magnetic medium [34]. These structures with spherical symmetry are hard to generate; therefore, the cylindrical Schwarzschild Black hole is considered in the next section.

3. REALIZATION OF CYLINDRICAL SCHWARZSCHILD BLACK HOLE

Under H. Chen, et al., suggestion, cylindrical back hole can be constructed with the following metric [29]:

$$ds^2 = -\left(1-\frac{L}{r}\right)dt^2 + \left(1-\frac{L}{r}\right)^{-1}dr^2 + r^2d\theta^2 + dz^2, \tag{22}$$

where by using relations (7), in the Cartesian coordinates, the permittivities are given by:

$$\varepsilon^{ij} = \mu^{ij} = \left(1-\frac{L}{r}\right)^{-1}\begin{pmatrix} 1-\frac{L}{r}\frac{x^2}{r^2} & -\frac{L}{r}\frac{xy}{r^2} & 0 \\ -\frac{L}{r}\frac{xy}{r^2} & 1-\frac{L}{r}\frac{y^2}{r^2} & 0 \\ 0 & 0 & 1 \end{pmatrix}, \tag{23}$$

In this case, the permittivities can be rewritten in the cylindrical coordinates as:

$$\varepsilon_r = \mu_r = 1, \quad \varepsilon_\theta = \mu_\theta = \varepsilon_z = \mu_z = \left(1-\frac{L}{r}\right)^{-1}. \tag{24}$$

As is evident, these parameters diverge, as r approaches the event horizon L. For considering the numerical solution, the following permittivity and permeability are considered:

$$\begin{aligned} &\mu_r = 1, \quad \mu_\theta = \varepsilon_z = \left(1-\frac{L}{r}\right)^{-1}, \quad r > L \\ &\mu_r = 1, \quad \mu_\theta = \varepsilon_z = \left(1-\frac{L'}{L}\right)^{-1}(1+i), \quad 0 < r < L, \end{aligned} \tag{25}$$

where $L' = L - \delta$ with $\delta \ll 1$, consequently, most of the TE electromagnetic waves are absorbed by the event horizon. Fig. 2 demonstrates the simulations for different incident Gaussian beams interacting with the metamaterial black hole. However, for realization of this device, we have at least two challenges: first, this device is infinitely large; second, it is constructed by anisotropic materials. To solve the first problem, we consider the following non-answer of Einstein's field equation:

$$ds^2 = -\alpha\left(1-\frac{L}{r}\right)dt^2 + \alpha^{-1}\left(1-\frac{L}{r}\right)^{-1}dr^2 + r^2d\theta^2 + dz^2, \tag{26}$$

where $\alpha = (1 - L/L_2)$ squeezes the space-time; in addition, we impose $\alpha(1 - L/r) = 1$ at $r = L_2$ while we suppose that the out of these regions, i.e., $r > L_2$, are flat; therefore, the above metric approaches the flat metric when r approaches L_2; according to this structures, the permittivity is given by

$$\varepsilon_r = \mu_r = 1, \quad \varepsilon_\theta = \mu_\theta = \varepsilon_z = \mu_z = \left(\alpha - \frac{\alpha L}{r}\right)^{-1}, \tag{27}$$

while outside $r = L_2$ is vacuum. To solve the second problem, by using the isotropic coordinates methods introduced in the Section 2, we obtain the isotropic transformed coordinates as

$$r(\tilde{r}) = \frac{(2\tilde{r}^\alpha + L)^2}{8\tilde{r}^\alpha}, \tag{28}$$

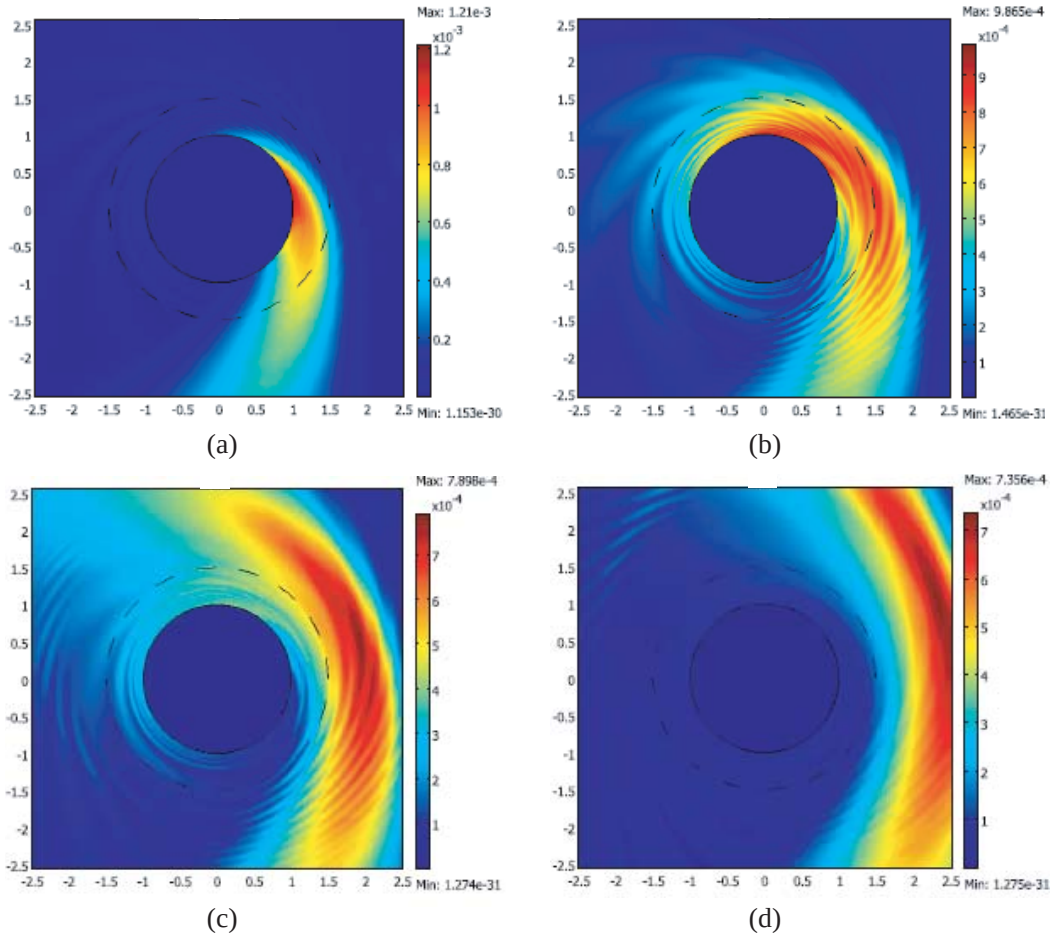

Figure 2. The magnetic field amplitude H near the black hole from Eq. (25) for different incident Gaussian beams with beam center at (a) $(2L, 0)$, (b) $(2.5L, 0)$, (c) $(3L, 0)$, (d) $(3.5L, 0)$. The incident wavelengths and the beam widths are $\lambda = \omega = 0.25L$. The beams are incident at an angle of 60 deg from x-axis [29].

where $\tilde{r}$ is the isotropic radial coordinate; consequently, the metric (26) is transformed as

$$ds^2 = -\left(\frac{2\tilde{r}^{\alpha} - L}{2\tilde{r}^{\alpha} + L}\right)^2 dt^2 + \left(\frac{(2\tilde{r}^{\alpha} + L)^2}{8\tilde{r}^{\alpha+1}}\right)^2 \left(dx^2 + dy^2 + dz^2\right). \tag{29}$$

Finally, by using the relation (7), the refractive index profile of the metric (29), is obtained as

$$n(\tilde{r}) = \frac{(2\tilde{r}^{\alpha} + L)^3}{8\tilde{r}^{\alpha+1}(2\tilde{r}^{\alpha} - L)}, \quad \tilde{r} \in \left[\left(\frac{L}{2}\right)^{1/\alpha}, \infty\right). \tag{30}$$

In this case, Fig. 1(d) shows the propagation of light for this structure, described by relation (30), with $L_2 = 5$ and $L = 1/2$.

4. OPTICAL BLACK HOLE

Another idea which has been theoretically and experimentally investigated in detail is optical black hole or attractor. Indeed, the idea of such a device is based on the Schwarzschild black hole even though it is not directly related to the transformation optics. This device, consists of the payload core with the radius R_c, surrounded by the concentrating shell of radius R, which was suggested and studied in

several works so far [18–25]. In this paper, we focus on the cylindrically symmetric distributions of the dielectric permittivity $\varepsilon(r)$ as follows:

$$\varepsilon(r) = \begin{cases} \varepsilon_0, & r > R \\ \varepsilon_0 \frac{R^2}{r^2}, & R_c < r < R, \\ \varepsilon_c + i\gamma, & r < R_c, \end{cases} \tag{31}$$

where $R_c = R\frac{\varepsilon_0}{\varepsilon_c}$. By using the geometrical optics, the effective Hamiltonian that describes the trace of light ray propagation is given by the relation (13). Fig. 3 shows the propagation of light for this structure, described by relation (31).

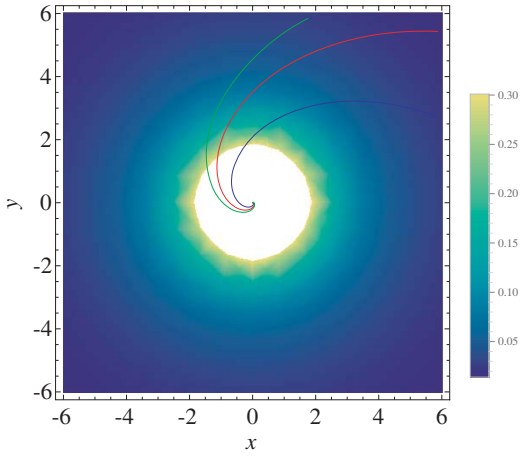

Figure 3. Density plots of refractive index of analogue medium of optical attractor (31) as well as propagation dynamics of light rays.

Moreover, by solving the Maxwell equations, directly, for TE polarization, i.e., $E = E(r,\phi)\hat{z}$, we can obtain

$$E(r,\phi,t) = e^{-im\phi - i\omega t} \begin{cases} AJ_m\left(\sqrt{\varepsilon_c + i\gamma}\frac{\omega}{c}r\right), & r < R_c, \\ B\cos\left[\sqrt{k_0^2R^2 - m^2}\log\frac{r}{R}\right] + C\sin\left[\sqrt{k_0^2R^2 - m^2}\log\frac{r}{R_c}\right], & R_c < r < R, \\ H_m^-(k_0r) + r_mH_m^+(k_0r), & r > R, \end{cases}$$

where A, B and C are constants; J_m and $H_m^{\pm} = J_m \pm iY_m$ are respectively the standard Bessel function and Hankel function; r_m is the reflection coefficient for the angular momentum m. By considering the boundary conditions, that is, continuity of E and its normal derivative, reflection coefficient r_m is given by

$$r_m = \frac{H_m^{-\prime}(k_0R) + \eta_m H_m^-(k_0R)}{H_m^{+\prime}(k_0R) + \eta_m H_m^+(k_0R)}, \tag{32}$$

where

$$\eta_m = -\frac{\sqrt{k_0^2R^2 - m^2}}{k_0R}\tan\left(\sqrt{k_0^2R^2 - m^2}\log\frac{R}{R_c} - \arctan\left(\frac{pk_0R}{\sqrt{k_0^2R^2 - m^2}}\right)\frac{J_m'(pk_0R)}{J_m(pk_0R)}\right), \tag{33}$$

and $p = \sqrt{(\varepsilon_c + i\gamma)/\varepsilon_0}$. In this case, the absorption cross section per unit length of a cylinder is obtained

$$\sigma_a = 2R\left[1 - 2F\left(\frac{k_0R\gamma}{\varepsilon_c}\right) + F\left(\frac{2k_0R\gamma}{\varepsilon_c}\right)\right], \tag{34}$$

where

$$F(x) = \int_0^{\pi/2} d\theta\cos\theta e^{-x\cos\theta} \approx \frac{1}{x^2}, \quad x \gg 1, \tag{35}$$

Therefore, as we expect, the absorption cross section per unit length, under the condition $k_0 R\gamma \gg 1$, is close to the full geometrical cross-section of the cylinder, $2R$ [23].

Also, by using the same method, the magnetic component of TM polarization electromagnetic waves are given by [58]

$$H_z^{in} = \sum_{n=-\infty}^{\infty} H_z^{in}(r) e^{in\phi - i\omega t} \quad R_c < r < R \tag{36}$$

in which n is the angular momentum number, ω is the angular frequency and $H_z^{in}(r)$ are given by

$$H_z^{in}(r) = A_n \left(\frac{r}{R}\right)^{-1+\sqrt{n^2-k_0^2R^2+1}} + B_n \left(\frac{r}{R}\right)^{-1-\sqrt{n^2-k_0^2R^2+1}}. \tag{37}$$

In addition, if we suppose that, for TM polarization electromagnetic waves, the Gaussian beam is incident [19],

$$H_z^{inc}(r,\phi;t) = \sum_{n=-\infty}^{\infty} P_n i^n J_n(k_0 r) e^{in\phi - i\omega t}, \quad r > R, \tag{38}$$

in which $J(k_0 r)$ are Bessel functions of order n and P_n obtained by [58, 59],

$$P_n = \frac{W_0}{2\sqrt{\pi}} \int_{-\infty}^{\infty} e^{\frac{1}{2}k_y^2 W_0^2 - i\sqrt{k^2-k_y^2}x_0 - ik_y y_0 - i\alpha n} dk_y, \tag{39}$$

where W_0 is half of the beam waist, (x_0, y_0) is beam center in Cartesian coordinates and $\alpha = \frac{2\pi}{\lambda}\sin^{-1}(\frac{k_y}{k})$. The total magnetic field H_z^{out} is the summation of the incident field and the scattering field H_z^{sca}, given by

$$H_z^{sca}(r,\phi;t) = \sum_{n=-\infty}^{\infty} Q_n i^n H_n^1(k_0 r) e^{in\phi - \omega t} \tag{40}$$

where H_n^1 is the first kind Hankel function [19]. In the region $R_c < r < R$, the magnetic fields are given by [58],

$$H_z^{in} = \sum_{n=-\infty}^{\infty} H_z^{in}(r) e^{in\phi - i\omega t} \quad R_c < r < R \tag{41}$$

in which n is the angular momentum number and ω the angular frequency. Finally, the magnetic fields in core region are given by [58],

$$H_z^{core}(r,\phi;t) = \sum_{n=-\infty}^{\infty} C_n J_n\left(k_0\sqrt{\varepsilon_c + i\gamma} r\right) e^{in\phi - i\omega t}. \tag{42}$$

In this case, the absorption cross section per unit length is given by [60],

$$\sigma_a = \frac{-4}{k_0} \sum_{-\infty}^{\infty} \left(\left|\frac{Q_n}{P_n}\right|^2 + \mathrm{Re}\left[\frac{Q_n}{P_n}\right] \right) \tag{43}$$

which is also close to the quantity of $2R$ [60].

For realization of the optical attractor device with permittivity (31), multilayered cylindrical structure is applied. The inhomogeneous region $R_c < r < R$ is divided into N concentric shells of isotropic dielectrics with equal thickness. The left panel of Fig. 4 shows the magnetic field intensity pattern for an incident Gaussian beam interacting with the EM black hole, which is calculated based on rigorous solutions Equations (37)–(42). The right panel of Fig. 4 indicates the magnetic field intensity pattern near the multi-layered EM black hole, with 12-layers, as a concrete example [19, 26]. In Ref. [19], an experimental work has been done with five kinds of real isotropic materials, including air, aluminum (Al) metal rods, polyethylene (PE), polymethyl methacrylate (PMMA) plexiglass, and polyvinylidene fluoride (PVDF) which their relative permittivities in microwave frequencies near 10 GHz are respectively about $\varepsilon_{air} = 1$, $\varepsilon_{Al} = \infty$, $\varepsilon_{PE} = 2.3$, $\varepsilon_{PMMA} = 2.6$ and $\varepsilon_{PVDF} = 7 + 0.7i$, with the thickness of each layer equal to 5 mm.

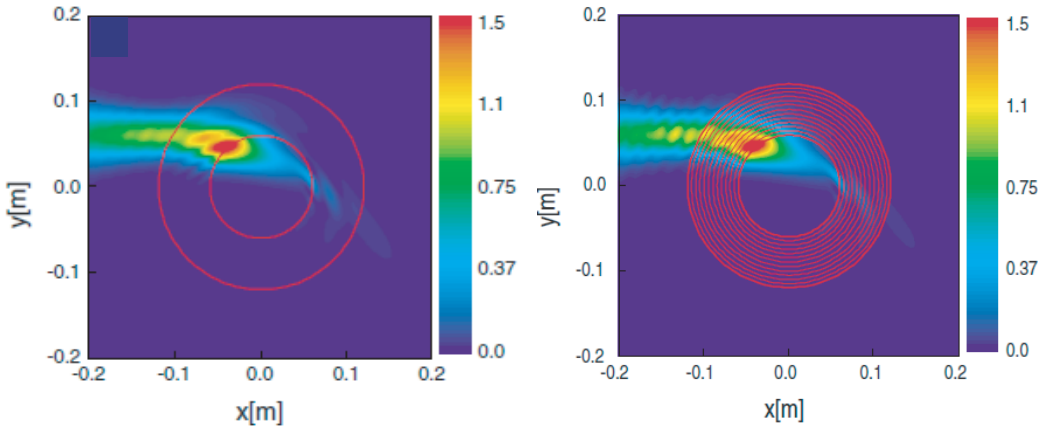

Figure 4. The left plot is shown the magnetic field intensity pattern for an incident Gaussian beam interacting with the EM black hole, which is calculated based on rigorous solutions Eqs. (37)–(42). The right plot indicates the magnetic field intensity pattern near the multi-layered EM black hole, with 12-layers with associated permittivities, respectively, $\varepsilon_1 = 3.66$, $\varepsilon_2 = 3.15$, $\varepsilon_3 = 2.60$, $\varepsilon_4 = 2.30$, $\varepsilon_5 = 2.12$, $\varepsilon_6 = 1.89$, $\varepsilon_7 = 1.66$, $\varepsilon_8 = 1.54$, $\varepsilon_9 = 1.41$, $\varepsilon_{10} = 1.34$, $\varepsilon_{11} = 1.28$, $\varepsilon_{12} = 1$ and their thickness is considered $d = 1\,\text{mm}$ [19].

Finally, we have to mention the possibility of construction of the omnidirectional absorbers by using a conformal mapping [16]. Indeed, by using the following conformal mapping:

$$w = Az^n, \quad A \neq 0, \quad n < 0, \tag{44}$$

in which $w = x' + iy'$ is the physical space and $z = x + iy$ is the virtual space, Z. Chang, et al., have constructed a omnidirectional absorbers for elastic waves [16].

5. REALIZATION OF THE SCHWARZSCHILD BLACK HOLE BY HYPERBOLIC METAMATERIALS

As is mentioned before, the hyperbolic metamaterials demonstrates the curved space-time, including (1 + 2)-Minkowski spacetime, back hole, wormhole, and two-times physics [38–45]. Indeed, one dimension, in the hyperbolic metamaterials, can be considered as a "time-like" coordinate whereas other dimensions indicate spatial coordinates [13, 14, 42]. It can be illustrated by considering a nonmagnetic uniaxial anisotropic metamaterial with dielectric permittivities $\varepsilon_x = \varepsilon_y = \varepsilon_1 > 0$ and $\varepsilon_z = \varepsilon_2 < 0$ that is added to this assumption that this behaviour holds in some frequency range around $\omega = \omega_0$. Therefore, any electromagnetic field propagating in this material can be considered as a sum of ordinary and extraordinary contributions, each of these being a sum of an arbitrary number of plane waves polarized in the ordinary $E_z = 0$ and extraordinary $E_z \neq 0$ directions [13, 14, 42]. Now, by considering scalar extraordinary wave function $E_z = \phi$, the ordinary portion of the electromagnetic field does not contribute to ϕ. Now, by considering Maxwell equations in frequency domain [61],

$$\frac{\omega^2}{c^2} D_\omega = \nabla \times \nabla \times E_\omega \quad D_\omega = \varepsilon E_\omega \tag{45}$$

the Klein-Gordon equation is obtained,

$$-\varepsilon_1^{-1} \partial_z^2 \phi_\omega + \varepsilon_2^{-1} \left(\partial_x^2 \phi_\omega + \partial_y^2 \phi_\omega \right) = \frac{\omega^2}{c^2} \phi_\omega, \tag{46}$$

in which the spatial coordinate $z = \tau$ behaves as a timelike coordinate. By this assumption, the z-dependent dielectric permittivity component $\varepsilon_z = \varepsilon_2$ changes sign at $z = 0$, the dielectric tensor of the composite is given by

$$\varepsilon_1 \approx \varepsilon_d, \quad \varepsilon_2 \approx \varepsilon_d + p(z)\varepsilon_m, \tag{47}$$

where $-\varepsilon_m \gg \varepsilon_d \sim 1$ and $p \ll 1$. By considering the in-plane wave vector (k_x, k_y), i.e.,

$$E_\omega(r) = E(z)e^{ik_x x + ik_y y}, \tag{48}$$

so that the ordinary and extraordinary waves correspond to the TE- and TM-polarized modes, respectively. We consider the case of constant $\varepsilon_2 = \varepsilon_z < 0$ and assume that finite $\varepsilon_1(x) = \varepsilon_x = \varepsilon_y$ changes sign from $\varepsilon_1 > 0$ to $\varepsilon_1 < 0$ as a function of x as is indicated in Fig. 5. Introducing $\psi = B$, we obtain [42]

$$-\partial_x^2\psi + \frac{\varepsilon_2}{\varepsilon_1}\partial_z^2\psi = \frac{\varepsilon_2\omega_0^2}{c^2}\psi, \tag{49}$$

where $E_x \sim -\varepsilon_x^{-1}\partial_x\psi$ diverges at the interface. By considering $\varepsilon_1 = \alpha x^2$, at $x = 0$ leads to Rindler-like optical space [62] near the interface, which is written as

$$ds^2 = -\frac{g^2x^2}{c^2}dt^2 + dl^2, \tag{50}$$

which can describe the area near the event horizon of the Schwarzschild Black hole [42]. Since the extraordinary photon wave vector $k \approx k_x \sim (\varepsilon_2/\varepsilon_1)^{1/2}k_z$ diverges at the interface, the optical length element of the extraordinary photons also diverges,

$$dl_{opt}^2 = \frac{k^2c^2}{\omega^2}dl^2 \sim \frac{dl^2}{x^2} \tag{51}$$

where the spatial line element dl corresponds to Fermat metric as perceived by the Rindler observers.

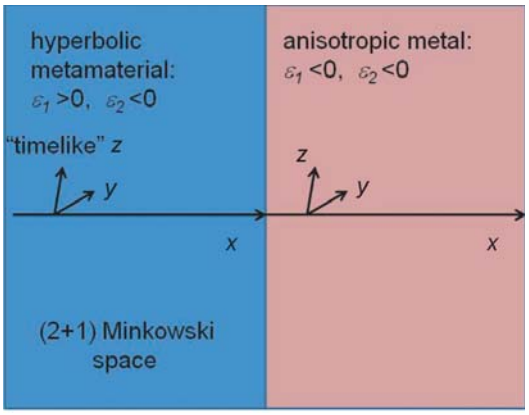

Figure 5. Metric signature change across a spacelike direction leads to appearance of a Rindler horizon [42].

6. CONCLUSIONS

Realization of celestial objects in the laboratory has been a tantalizing concept for human being over centuries. Recent developments in transformation optics as well as metamaterial science have caused the extension of a multidisciplinary field, including general relativity, quantum gravity, inflation and string theory on the one hand, and optics and metamaterial science, on the other. Indeed, realization of some experimental works about two times physics, string theory, quantum gravity and inflation as well as realization some celestial objects, such as black hole, worm hole and FRW universe, Gödel metric and multiuniverse, in the laboratory have been a result of these progresses. In this review paper, we investigated some realizations of black holes in optics as the interesting object in theoretical physics. For this purpose, we started with the Maxwell equations in curved space-time; then, with a brief review of isotropic coordinates transformation method, we considered the refractive index of such structures and investigated the propagations of light ray in these cases, including Schwarzschild and linearized black holes as well as cylindrical ones. Optical attractor, as another case which can be realized in technological applications, was investigated. Finally, our particular attention was devoted to the Rindler space-time, as a one dimension black hole, in the last part of this review.

ACKNOWLEDGMENT

The authors gratefully acknowledge Mr. Joseph Bass, University of North Florida (UNF), for some useful discussions and editing of this paper. This work was sponsored by the National Natural Science Foundation of China under Grants No. 61322501, No. 61574127, No. 61275183, and No. 61550110245 the Top-Notch Young Talents Program of China, the Program for New Century Excellent Talents (NCET-12-0489) in University, the Fundamental Research Funds for the Central Universities, and the Innovation Joint Research Center for Cyber-Physical-Society System.

REFERENCES

1. Butterfielf, J. and J. Earman, *Philosophy of Physics, Part A*, Elsevier, North-Holland, 2007.
2. Landy, N. I., S. Sajuyigbe, J. J. Mock, D. R. Smith, and W. J. Padilla, "Perfect metamaterial absorber," *Phys. Rev. Lett.*, Vol. 100, 207402, 2008.
3. Atwater, H. A. and A. Polman, "Plasmonics for improved photovoltaic devices," *Nature Mater.*, Vol. 9, 205, 2010.
4. Schuller, J. A., E. S. Barnard, W. Cai, Y. C. Jun, J. S. White, and M. L. Brongersma, "Plasmonics for extreme light concentration and manipulation," *Nature Mater.*, Vol. 9, 193, 2010.
5. Pendry, J. B., "Controlling light on the nanoscale (invited review)," *Progress In Electromagnetics Research*, Vol. 147, 117–126, 2014.
6. Ward, A. J. and J. B. Pendry, "Refraction and geometry in Maxwell's equations," *Journal of Modern Optics*, Vol. 43, 773, 1996.
7. Schurig, D., J. B. Pendry, and D. R. Smith, "Calculation of material properties and ray tracing in transformation media," *Optics Express*, Vol. 14, 9794, 2006.
8. Pendry, J. B., D. Schurig, and D. R. Smith, "Controlling electromagnetic fields," *Science*, Vol. 312, 1780, 2006.
9. Leonhardt, U., "Optical conformal mapping," *Science*, Vol. 312, 1777, 2006.
10. Sheng, C., H. Liu, Y. Wang, S. N. Zhu, and D. A. Genov, "Trapping light by mimicking gravitational lensing," *Nat. Photonics.*, Vol. 7, 902, 2013.
11. Genov, D. A., "Optical black-hole analogues," *Nat. Photonics.*, Vol. 5, 76, 2011.
12. Reznik, B., "Origin of the thermal radiation in a solid-state analogue of a black hole," *Phys. Rev. D*, Vol. 62, 044044, 2000.
13. Smolyaninov, I. and Y. J. Hung, "Modeling of time with metamaterials," *J. Opt. Soc. Am. B*, Vol. 28, 1591, 2011.
14. Smolyaninov, I. and E. E. Narimanov, "Metric signature transitions in optical metamaterials," *Phys. Rev. Lett.*, Vol. 105, 067402, 2010.
15. Teixeira, F. L. and W. C. Chew, "Differential forms, metrics, and the reflectionless absorption of electromagnetic waves," *Journal of Electromagnetic Waves and Applications*, Vol. 13, No. 5, 655–686(22), 1999.
16. Chang, Z. and G. Hu, "Elastic wave omnidirectional absorbers designed by transformation method," *Applied Phys. Lett.*, Vol. 101, 054102, 2012.
17. Leonhardt, U. and T. G. Philbin, "General relativity in electrical engineering," *New J. Phys.*, Vol. 8, 247, 2006.
18. Odabasi, H., F. L. Teixeira, and W. C. Chew, "Impedance-matched absorbers and optical pseudo black holes," *J. Opt. Soc. Am. B*, Vol. 5, 1317, 2011.
19. Lu, W., J. Jin, Z. Lin, and H. Chen, "A simple design of an artificial electromagnetic black hole," *J. App. Phys.* Vol. 108, 064517, 2010.
20. Cheng, Q., T. J. Cui, W. X. Jiang, and B. G. Cai, "An omnidirectional electromagnetic absorber made of metamaterials," *New J. Phys.*, Vol. 12, 063006, 2010.
21. Argyropoulos, C., E. Kallos, and Y. Hao, "FDTD analysis of the optical black hole," *J. Opt. Soc. Am. B*, Vol. 10, 2020, 2010.

22. Wang, H.-W. and L.-W. Chen, "Wide-angle absorber achieved by optical black holes using graded index photonic crystals," *J. Opt. Soc. Am. B*, Vol. 8, 2222, 2012.
23. Narimanov, E. E. and A. V. Kildishev, "Optical black hole: Broadband omnidirectional light absorber," *Applied Phys. Lett.*, Vol. 95, 041106, 2009.
24. Lee, Y. Y., E. S. Kang, K. H. Jung, J. W. Lee, and D. Ahn, "Elliptic cylindrical pseudo-optical black hole for omnidirectional light absorber," *J. Opt. Soc. Am. B*, Vol. 8, 1948, 2014.
25. Prokopeva, L. J., E. E. Narimanov, and A. V. Kildishev, "Elliptic cylindrical pseudo-optical black hole for omnidirectional light absorber: Comment," *J. Opt. Soc. Am. B*, Vol. 4, 719, 2015.
26. Kildishev, A. V., L. J. Prokopeva, and E. E. Narimanov, "Cylinder light concentrator and absorber: Theoretical description," *Opt. Express*, Vol. 18, 16646, 2010.
27. Qiu, J., J. Y. Tan, L. H. Liu, and P.-F. Hsu, "Infrared radiative properties of two-dimensional square optical black holes," *Journal of Quantitative Spectroscopy & Radiative Transfer*, Vol. 112, 2584, 2011.
28. Mackay, T. G. and A. Lakhtakia, "Towards a metamaterial simulation of a spinning cosmic string," *Phys. Lett. A*, Vol. 374, 2305, 2010.
29. Chen, H., R.-X. Miao, and M. Li, "Transformation optics that mimics the system outside a Schwarzschild black hole," *Opt. Exp.*, Vol. 14, 15183, 2010.
30. Genov, D. A., S. Zhang, and X. Zhang, "Mimicking celestial mechanics in metamaterials," *Nat. Phys.*, Vol. 5, 687, 2009.
31. Khorasani, S. and B. Rashidian, "Optical anisotropy of schwarzschild metric within equivalent medium framework," *Optics Communications*, Vol. 283, 1222, 2010.
32. Nerkararyan, K. V., S. K. Nerkararyan, and S. I. Bozhevolnyi, "Plasmonic black-hole: broadband omnidirectional absorber of gap surface plasmons," *Opt. Lett.*, Vol. 22, 4311, 2011.
33. Qiu, J., J. Y. Tan, L. H. Liu, and P.-F. Hsu, "Radiative properties of optical board embedded with optical black holes," *Journal of Quantitative Spectroscopy & Radiative Transfer*, Vol. 112, 832, 2011.
34. Mackay, T. G. and A. Lakhtakia, "Towards a realization of Schwarzschild-(anti-)de Sitter spacetime as a particulate metamaterial," *Phys. Rev. B*, Vol. 83, 195424, 2011.
35. Smolyaninov, I. I., "Virtual black holes in hyperbolic metamaterials," Arxive: 1101.4625, 2011.
36. Zhang, Y.-L., X.-Z. Dong, M.-L. Zheng, Z.-S. Zhao, and X.-M. Duan, "Steering electromagnetic beams with conical curvature singularities," *Opt. Lett.*, Vol. 40, 4784, 2015.
37. Boston, B. R., "Time travel in transformation optics: Metamaterials with closed null geodesics," *Phys. Rev. D.*, Vol. 91, 124035, 2015.
38. Smolyaninov, I., "Hyperbolic metamaterials," arXive: 1510.07137, 2015.
39. Smolyaninov, I., E. Hwang, and E. E. Narimanov, "Hyperbolic metamaterial interfaces: Hawking radiation from Rindler horizons and spacetime signature transitions," *Phys. Rev. D*, Vol. 85, 235122, 2012.
40. Smolyaninov, I., "Surface plasmon toy model of a rotating black hole," *New J. Phys.*, Vol. 5, 147, 2003.
41. Smolyaninov, I., "Critical opalescence in hyperbolic metamaterials," *J. Opt.*, Vol. 13, 125101, 2011.
42. Smolyaninov, I., E. Hwang, and E. Narimanov, "Hyperbolic metamaterial interfaces: Hawking radiation from Rindler horizons and spacetime signature transitions," *Phys. Rev. B*, Vol. 85, 235122, 2012.
43. Smolyaninov, I. and Y. Hung, "Minkowski domain walls in hyperbolic metamaterials," *Phys. Lett. A*, Vol. 373, 353, 2013.
44. Smolyaninov, I., "Quantum electromagnetic black holes in a strong magnetic field," *J. Phys. G: Nucl. Part. Phys.*, Vol. 40, 015005, 2013.
45. Smolyaninov, I., Y. Hung, and E. Hwang, "Experimental modeling of cosmological inflation with metamaterials," *Phys. Lett. A*, Vol. 376, 2575, 2012.

46. Kinsler, P. and M. W. McCall, "The futures of transformations and metamaterials," *Photon. Nanostruct. Fundam. Appl.*, Vol. 15, 10, 2015.
47. McCall, M. W., A. Favaro, P. Kinsler, and A. Boardman, "A spacetime cloak, or a history editor," *J. Opt.*, Vol. 13, 024003, 2011.
48. Kinsler, P. and M. W. McCall, "Transformation devices: carpets in space and space-time," *Phys. Rev. A*, Vol. 81, 063818, 2014.
49. Halimeh, J. C., R. T. Thompson, and M. Wegener, "Invisibility cloaks in relativistic motion," arXive: 1510.06144, 2015.
50. Susskind, L. and J. Lindesay, *An Introduction to Black Holes, Information and the String Theory Revolution*, World Scientific, Singapore, 2005.
51. Leonhardt U., "On cosmology in the laboratory," *Phil. Trans. R. Soc. A*, Vol. 373, 20140354, 2015.
52. Faccio, D., F. Belgiorno, S. Cacciatori, V. Gorini, S. Liberati, and U. Moschella, *Analogue Gravity Phenomenology: Analogue Spacetimes and Horizons, from Theory to Experiment*, Springer, Switzerland, 2013.
53. Gron, O. and S. Hervik, *Einsteins General Theory of Relativity*, Springer, New York, 2007.
54. Leonhardt, U. and T. G. Philbin, *Geometry and Light: The Science of Invisibility*, Dover, Mineola, NY, 2010.
55. Misner, C. W., K. Thorne, and J. A. Wheeler, *Gravitation*, W. H. Freeman and Company, New York, 1973.
56. Landau, L. and E. M. Lifshitz, *The Classical Theory of Fields*, Elsevier, Oxford, 2000.
57. Padmanabhan, T., *Gravitation*, Cambridge University Press, Cambridge, 2010.
58. Kaliteevski, M. A., R. A. Abram, V. V. Nikolaev, and G. S. Sololovski, "Bragg reflectors for cylindrical waves," *J. Mod. Opt.*, Vol. 46, 875, 1999.
59. Zimmermann, E., R. Dandliker, and N. Souli, "Scattering of an off-axis Gaussian beam by a dielectric cylinder compared with a rigorous electromagnetic approach," *J. Opt. Soc. Am.*, Vol. 12, 398, 1995.
60. Bohren, C. F. and D. R. Huffman, *Absorption and Scattering of Light by Small Particles*, Wiley, New York, 1983.
61. Landau, L. and E. Lifshitz, *Electrodynamics of Continuous Media*, Elsevier, Oxford, 2004.
62. Dehdashti, S., R. Roknizadeh, and A. Mahdifar, "Analogue special and general relativity by optical multilayer thin films: the Rindler space case," *J. Mod. Opt.*, Vol. 60, 233, 2013.